Lukas Nejdl[1]
Miguel Angel Merlos Rodrigo[2]
Jiri Kudr[1,2]
Branislav Ruttkay-Nedecky[2]
Marie Konecna[2]
Pavel Kopel[2]
Ondrej Zitka[1,2]
Jaromir Hubalek[2]
Rene Kizek[2]
Vojtech Adam[1,2]

[1]Department of Chemistry and Biochemistry, Faculty of Agronomy, Mendel University in Brno, Brno, Czech Republic
[2]Department of Microelectronics, Faculty of Electrical Engineering and Communication, Central European Institute of Technology, Brno University of Technology, Brno, Czech Republic

Received April 21, 2013
Revised June 19, 2013
Accepted June 19, 2013

Research Article

Liposomal nanotransporter for targeted binding based on nucleic acid anchor system

Microfluidic techniques have been developed intensively in recent years due to lower reagent consumption, faster analysis, and possibility of the integration of several analytical detectors into one chip. Electrochemical detectors are preferred in microfluidic systems, whereas liposomes can be used for amplification of the electrochemical signals. The aim of this study was to design a nanodevice for targeted anchoring of liposome as transport device. In this study, liposome with encapsulated Zn(II) was prepared. Further, gold nanoparticles were anchored onto the liposome surface allowing binding of thiol moiety-modified molecules (DNA). For targeted capturing of the transport device, DNA loops were used. DNA loops were represented by paramagnetic microparticles with oligo$(DT)_{25}$ chain, on which a connecting DNA was bound. Capturing of transport device was subsequently done by hybridization to the loop. The individual steps were analyzed by electrochemistry and UV/Vis spectrometry. For detection of Zn(II) encapsulated in liposome, a microfluidic system was used. The study succeeded in demonstrating that liposome is suitable for the transport of Zn(II) and nucleic acids. Such transporter may be used for targeted binding using DNA anchor system.

Keywords:
Gold nanoparticles / Liposome / Microfluidic / Nanomedicine / Nucleic acids / Paramagnetic particles
DOI 10.1002/elps.201300197

1 Introduction

Microfluidic techniques and devices have rapidly developed in recent years due to lower reagent consumption, and faster and more sensitive analysis [1, 2]. The production of these devices is of low cost and allows to integrate several steps of analysis process into a chip [3]. Numerous diagnostic applications of microfluidic techniques associated with genes, proteins, and cells have been described in accordance to the advantages related with miniaturization, automation, sensitivity, and specificity [4–10]. Considerable innovation was achieved by coupling these methods with approaches of molecular biology and immunochemistry to form biosensors [1, 11–15].

Electrochemical detection integrated in microfluidic system is preferred in comparison with optical detection due to the easier and cheaper instrumentation and its versatility [12]. Electrochemical analysis is one of the most sensitive methods for determination of inorganic and also organic substances, however determination of different analytes in biological matrix can be influenced by interferences and the sensitivity is not sufficient. To enhance electrochemical signal, nanoparticles and magnetic microparticles can be used [16, 17]. Application of liposomes, member of nanoparticle-based materials, is advantageous for this purpose. In this case, electroactive reagent is controlled, released from liposome, and determined [16, 18]. Liposomes, sphere-shaped vesicles, are composed of a phospholipid bilayer surrounding an aqueous core [19, 20]. The inner cavity of the liposomes can be used for storage of enzymes, proteins, DNA, drugs, and other substances [21–26]. Research on liposome technology has progressed from conventional vesicles to second-generation liposomes, in which long-circulating liposomes are obtained by modulating the lipid composition, size, and charge of the vesicle. The membrane of these spherical bodies can be modified by various bioactive substances to achieve specific interactions. The most applied modifications of liposomal membrane are based on antibodies, protein receptors, and radiolabeling [27–29]. Numerous sensitive voltammetric methods are based on the presence of electroactive compound in the cavity of the liposome [14, 15, 30, 31]. Zhong

Correspondence: Dr. Vojtech Adam, Department of Chemistry and Biochemistry, Faculty of Agronomy, Mendel University in Brno, Zemedelska 1, CZ-613 00 Brno, Czech Republic
E-mail: vojtech.adam@mendelu.cz
Fax: +420-5-4521-2044

Abbreviations: **AAS**, atomic absorption spectrometry; **AuNP**, gold nanoparticle; **DPV**, differential pulse voltammetry; **LipoZn**, liposome with encapsulated Zn; **MB**, magnetic bead; **MP**, magnetic particle; **Nitro-PAPS**, 2-(5-brom-2-pyridylazo)-5-(*N*-propyl-*N*-sulfopropylamino)-phenol; **ODN**, oligodeoxynucleotides; **ODN-SH**, thiolated ODN

Colour Online: See the article online to view Figs. 1–5 in colour.

et al. constructed a multiplex immunoassay based on the amplification strategy using the liposomes, which contained electrochemical active molecules (ascorbic acid and uric acid) as signal enhancers for the simultaneous detection of neuron-specific enolase and pro-gastrin-releasing peptide [14]. Similarly, Viswanathan et al. described a sensitive method for detection of cholera toxin by using an electrochemical immunosensor with liposomic magnification followed by adsorptive square-wave stripping voltammetry [15]. Potassium ferrocyanide-encapsulated and ganglioside-functionalized liposomes act as highly specific recognition labels for the amplified detection of cholera toxin. By this way, it is possible to indirectly detect the compounds specifically bounded in the liposome structure. The first step is preparation of liposome with encapsulated metal and bound DNA on its surface. For the detection of metal, it is necessary to "open" the liposome structure by using detergent or an electric field [32–34].

In this study, we focused on the preparation of nanodevices for targeted liposomal transport utilizing nucleic acids chains. Liposome with encapsulated Zn(II) (lipoZn) was prepared. On the surface of the liposome, gold nanoparticles (AuNPs) were anchored, which allowed binding of thiol moiety (SH)-modified DNA molecules. For targeted capturing of the transport device, DNA loops were used. DNA loops were represented by paramagnetic microparticles with oligo$(DT)_{25}$ chain, on which a connecting DNA was bound. Capturing of transport device was subsequently done by hybridization to the loop. Each step was analyzed by electrochemistry and subsequently by UV/Vis spectrometry.

2 Materials and methods

2.1 Chemicals and materials

Cholesterol, 1,2-dioleoyl-sn-glycero-3-phospho-rac-(1-glycerol) sodium salt, chloroform, $Zn(NO_3)_2 \cdot 6H_2O$, sodium citrate, $HAuCl_4 \cdot 3H_2O$, and water were purchased from Sigma-Aldrich (St. Louis, MO, USA) in ACS purity, unless noted otherwise. Hydrogenated phosphatidylcholine from soybean was a gift from Lipoid (Ludwigshafen, Germany). Magnetic particles (MPs) oligo$(DT)_{25}$ were purchased from Invitrogen (Oslo, Norway). To pipette volumes down to microliters, pipettes were purchased from Eppendorf Research (Hamburg, Germany) with the highest certified deviation (±12%). The DI water was prepared using reverse osmosis equipment Aqual 25 (Aqual, Brno, Czech Republic). The DI water was further purified by using apparatus MiliQ Direct QUV equipped with the UV lamp. The resistance was 18 MΩ. The pH was measured using pH meter WTW inoLab (WTW, Weilheim, Germany).

2.2 Preparation of AuNPs

Gold nanoparticles were prepared by citrate method at room temperature according to Kimmling et al. and Polte et al. [35, 36]. Briefly, an aqueous solution of sodium citrate (0.5 mL, 40 mM) was added to a solution of $HAuCl_4 \cdot 3H_2O$ (10 mL, 1 mM). The color of the solution slowly changed from yellow to violet. Mixture was stirred overnight.

2.3 Preparation of liposome film and liposome filled with Zn(II) (lipoZn)

Liposome was prepared according to published method [37] with modification. Briefly, cholesterol (100 mg), 1,2-dioleoyl-*sn*-glycero-3-phospho-rac-(1-glycerol) sodium salt (100 mg), and phosphatidylcholine (100 mg) were dissolved in chloroform (4.5 mL). A lipid film was obtained by rotary evaporation of chloroform. Residual chloroform was removed by a stream of nitrogen. Solutions containing 0.25, 0.5, 1, and 2 mg of Zn(II) were added to lipid film (20 mg). Samples were homogenized with Ultra–Turrax T8 (IKA Werke, Staufen, Germany) for 10 min. The homogenized mixtures were then heated and shaken for 15 min at 60°C at Thermomixer Comfort (Eppendorf). The samples were then washed several times with MilliQ water on Amicon 3k (Merck Millipore, Merck, Darmstadt, Germany). Final volume of samples was 1 mL.

2.4 Modification of liposome surface by AuNPs and thiolated oligodeoxynucleotides (ODN-SH)

Modification of liposomes was done according to Bhuvana et al. [38]. One milliliter of water containing 1 mg of Zn(II) was added to liposome (20 mg), homogenized, and heated as described in the Section 2.3. After cooling, 1 mM solution (500 μL) of AuNPs was added. The mixture was shaken for 3 h on Biosan Orbital Shaker OS-10 (Biosan, Riga, Latvia). Subsequently, volume was reduced on Amicon 3K (3500 rpm, 20°C, 15 min). The mixture was washed several times with MiliQ water and finally diluted to 1 mL. Thirty microliters of thiolated synthetic ODNs (ODN-SH) was mixed with 30 μL of modified liposome and incubated for 1.5 h on Multi RS-60 (Biosan). The sequence of ODN-SH was 5′ CTGGAATGCAGA(SH) 3′ (Sigma-Aldrich). This probe was complementary to target oligodeoxynucleotide probe (5′ TCTGCATTCCAGAAAAA, Sigma-Aldrich), which was anchored to paramagnetic microparticles (MPs) oligo$(DT)_{25}$, 3.3×10^8 beads/mL (Invitrogen, Oslo, Norway).

2.5 Isolation of nanogold-modified liposomes using magnetic microparticles

For isolation of nanogold-modified liposomes, MPs oligo$(DT)_{25}$ were used. The solutions used for washing MPs were as follows: phosphate buffer I—0.1 M NaCl, 0.05 M Na_2HPO_4, 0.05 M NaH_2PO_4. The hybridization solutions were as follows: 0.1 M Na_2HPO_4, 0.1 M NaH_2PO_4, 0.6 M guanidinium thiocyanate (Amresco, Solon, OH, USA), 0.15 M Tris-HCl (pH 7.5), 0.2 M NaCl. The elution solutions were as follows: phosphate buffer II—0.2 M NaCl, 0.1 M Na_2HPO_4, 0.1 M NaH_2PO_4. For the first hybridization, 10 μL

of (MPs) oligo$(DT)_{25}$ was pipetted to Eppendorf tube on magnet and washed three times with 100 μL of phosphate buffer I. Afterward, 10 μL of ODN 5′ TCTG CATTCCAGAAAAA and 10 μL of hybridization buffer were added and incubated (30 min, 25°C) on Multi RS-60. Sample was washed three times with 100 μL of phosphate buffer I on magnet. The next step was second hybridization with 10 μL of lipoZn-AuNPs-ODN-SH mixed with 10 μL of hybridization buffer. The mixture was incubated (30 min, 25°C) and washed on magnet three times with phosphate buffer I (3 × 100 μL). Afterward, 40 μL of elution buffer (phosphate buffer II) was added and incubated (5 min, 85°C, 350 rpm) on Thermomixer Comfort. Magnetic particles were separated by magnet and solution was used for measurements. Other experimental details can be found in the following papers [39–43].

2.6 UV/Vis spectrophotometry

Spectra were recorded within the range from 220 to 800 nm on spectrophotometer SPECORD 210 (Analytik Jena, Jena, Germany) using quartz cuvettes (1 cm, Hellma, Essex, UK). Cuvette space was tempered by a Julabo thermostat (Labortechnik, Wasserburg, Germany) to temperature 25°C. Pipetted amount of reagent was 800 or 900 μL. Pipetted amounts of samples were 8, 9, and 40 μL. Spectra were recorded after 5 min-long incubation of a reagent with a sample. After measurement, cuvettes were rinsed with DI water and dried with nitrogen.

For spectral analysis of zinc, Zinc kit (Greiner Diagnostic, Bahlingen, Germany) was used. Zinc forms red chelate complex with 2-(5-brom-2-pyridylazo)-5-(*N*-propyl-*N*-sulfopropylamino)-phenol (Nitro-PAPS) with absorption maximum at $\lambda = 560$ nm. The color intensity is proportional to concentration of total zinc in the sample. 800 μL of reagent (Greiner Diagnostic, 0.02 mM Nitro-PAPS, 170 mM sodium citrate, 4 mM dimethylglyoxime, 1% detergent in 200 mM bicarbonate buffer, pH 9.8) was pipetted into plastic cuvette and subsequently 40 μL of the sample was added. Spectra were recorded at 25°C after 5 min-long incubation of a reagent with a sample. For spectral analysis of phosphorus, Phosphorus kit (Greiner Diagnostic) was used. Inorganic phosphorus reacts with ammonium molybdate in acidic medium to form a colored phosphomolybdic complex with absorption maximum at $\lambda = 340$ nm. 900 μL of reagent (Greiner Diagnostic, 210 mM sulfuric acid, 400 μM ammonium molybdate) was pipetted into plastic cuvettes and subsequently 9 μL of the sample was added. Spectra were recorded at 25°C after 5 min-long incubation of a reagent with a sample. For spectral analysis of cholesterol, Cholesterol kit (Greiner Diagnostic) was used. The principle of the enzymatic method for cholesterol determination by use of a single reagent is described briefly. Cholesterol esters in liposome are hydrolyzed to free cholesterol-by-cholesterol esterase (EC 3.1.1.13). The free cholesterol produced is oxidized by cholesterol oxidase (EC 1.1.3.6) to cholest-4-en-3-one with simultaneous production of hydrogen peroxide, which oxidatively couples with 4-aminoantipyrine and phenol in the presence of peroxidase (EC 1.11.1.7) to yield a chromogen with maximum absorption at 500 nm. The enzymatic method is divided into three enzymatic reactions. The substrate in the first reaction is cholesterol ester in liposome and corresponding enzyme is cholesterol esterase (200 U/L). The product from the first reaction, free cholesterol, is the substrate for the second reaction and corresponding enzyme is cholesterol oxidase (100 U/L). The product from the second reaction, hydrogen peroxide, is the substrate for the third reaction and corresponding enzyme is peroxidase (3.0 kU). All three enzymes are part of one reagent. 800 μL of reagent (Greiner Diagnostic, 0.3 mM 4-aminoantipyrin, 5 mM phenol, 3.0 kU/L peroxidase, 200 U/L cholesterol esterase, 100 U/L cholesteroloxidase in 50 mM Good's buffer, pH 6.7) was pipetted into plastic cuvette and subsequently 8 μL of the sample was added. Spectra were recorded at 25°C after 5 min-long incubation of a reagent with a sample.

2.7 Three-electrode system

2.7.1 Electrode system design

Electrode system was designed and fabricated as a disposable planar three-electrode sensor in LabSensNano laboratories of Brno University of Technology, Czech Republic. The electrodes shape and theoretical working area were designed according to the previous optimization [44]. In accordance with the optimization results, the working electrode was designed to be as large as possible (in this case, geometrically comparable with 3 mm diameter glassy carbon electrode with working area of 7.1 mm^2), reference electrode 1.3 mm^2, and auxiliary electrode 6.2 mm^2. Screen-printed sensor was fabricated using Aurel C880 semiautomatic screen-printer (Aurel Automation, Modigliana, Italy) and fired using BTU fast fire furnace for thick-film processing (BTU, North Billerica, USA). The conductive layer was fabricated from AgPdPt-based paste (Electroscience (ESL) 9562-G). The protective layer was fabricated from dielectric paste (ESL 4917). Auxiliary electrode was fabricated from Pt-based paste (ESL 5545). All cermet pastes were obtained from ESL ElectroScience Europe (Berkshire, UK) and fired at 850°C according to the recommended values in products datasheets. Working electrode was screen-printed using special carbon paste for electrodes of electrochemical sensors (DuPont BQ221) from DuPont Company (Wilmington, USA) and cured at 130°C for 10 min according to datasheet. Reference electrode was screen-printed using special polymer Ag/AgCl paste (DuPont 5874; Ag/AgCl ratio, 65:35) and dried at 120°C for 5 min. Other experimental details of the electrode fabrication can be found in Chudobova et al. [45].

2.7.2 Differential pulse voltammetry (DPV)

Printed three-electrode system was coupled with the flow cell according to the following scheme. The sample was

pumped using peristaltic pump (Amersham Biosciences, Uppsala, Sweden). Change of oxidative signal was recorded with potentiostat PGSTAT 101 (Metrohm, Herisau, Switzerland), and the results were evaluated by the software NOVA 1.8 (Metrohm). Potentiostat settings were as follows: initial potential −1.7 V, end potential −0.1 V, step potential 0.01 V, modulation amplitude 0.1 V, modulation time 0.004 s, interval time 0.1 s, equilibration time 40 s. Samples were diluted with acetate buffer pH 5 and measured at temperature 25°C.

2.7.3 Amperometry

Printed three-electrode system was coupled with the flow cell according to the following scheme. The sample was pumped using peristaltic pump (Amersham Biosciences). Change of oxidative signal was recorded with potentiostat PGSTAT 101 (Metrohm), and the results were evaluated by the software NOVA 1.8 (Metrohm). Potentiostat settings were as follows: wait time 5 s, duration 5 s, interval time 0.05 s, potential −1.6, −1.5, −1.4, −1.3, −1.25, −1.15, −1.1, −0.9, −0.8, −0.7, −0.6, and −0.5 V. Samples were diluted with acetate buffer, pH 5, and measured at temperature 25°C.

2.7.4 Square-wave voltammetric determination of ODN

Determination of ODN was performed with 663 VA Stand (Metrohm) with a conventional three-electrode configuration. A hanging mercury drop electrode was working electrode with drop area of 0.4 mm^2, Ag/AgCl/3M KCl was the reference electrode, and glassy carbon auxiliary electrode. Square-wave voltammetric measurements were carried out under the following parameters: deoxygenating with argon, 120 s; start potential, 0 V; end potential, −1.8 V; amplitude, 0.025 V; voltage step, 5 mV; equilibration time, 5 s; frequency, 280 Hz. Acetate buffer (0.2 M, pH 5.0) was used as the supporting electrolyte. Characteristic peak for ODN was observed at potential −1.4 V. The parameters were adopted from Huska et al. [39].

2.8 Atomic absorption spectrometry (AAS)

Determination of zinc was carried out on 240FS Agilent Technologies atomic absorption spectrometer (Santa Clara, USA) with flame atomization. The zinc hollow cathode lamp (Agilent) was operated at the current of 5 mA. Zinc was measured on the primary wavelength 213.9 nm with spectral bandwidth of 1.0 nm. The mixture of air and acetylene was used for flame atomization. Deuterium background correction was used and the signal was measured in the integration mode for 2 s. Gold was determined on 280Z Agilent Technologies atomic absorption spectrometer with electrothermal atomization. Gold ultrasensitive hollow cathode lamp (Agilent) was used as the radiation source. The spectrometer was operated at 242.8 nm resonance line with spectral bandwidth of 1.0 nm and the lamp current of 4 mA. The sample volume 20 μL was injected into the tube and the heating time-temperature program was on. The pyrolysis temperature 500°C for 8 s and the atomization temperature 2600°C for 3 s were applied. The flow of argon inert gas was 300 mL/min. After the atomization, the cleaning step was inserted (2800°C, 2 s) for total residue removal. Zeeman background correction was used with field strength 0.8 T. The absorption signal was evaluated in peak height mode with seven-point smoothing. Each sample was measured in three replicates.

2.9 Characterization of liposomes by MALDI-TOF MS analysis

The MS experiments were performed on a MALDI-TOF/TOF mass spectrometer Bruker Ultraflextreme (Bruker Daltonik, Bremen, Germany) equipped with a laser operating at wavelength of 355 nm with an accelerating voltage of 25 kV, cooled with nitrogen, and a maximum energy of 36 μJ with repetition rate 2000 Hz in reflector positive ion mode, and with software for data acquisition and processing of mass spectra flexControl version 3.4 and flexAnalysis version 2.2. 2,5-dihydroxybenzoic acid (Bruker) was used as the matrix. Twenty milligrams per milliliters of 2,5-dihydroxybenzoic acid was prepared in TA30 (30% ACN and 0.1% trifluoroacetic acid). Working standard solutions were prepared daily by dilution of the stock solutions. The solutions for analysis were mixed in ratio of 1:1 (matrix/sample). After obtaining a homogeneous solution, 1 μL was applied on the target and dried under atmospheric pressure and ambient temperature. Samples were spotted on MTP 384 target plate polished steel T F (Bruker Daltonik). A mixture of peptide calibrations standard (Bruker Daltonik) was used to externally calibrate the instrument. Mass spectra were typically acquired by averaging 20 subspectra from a total of 500 shots of the laser (Smartbeam 2, version: 1_0_38.5).

2.10 Descriptive statistics

Data were processed using MICROSOFT EXCEL® (USA) and STATISTICA.CZ version 8.0 (Czech Republic). Results are expressed as mean ± SD unless noted otherwise (EXCEL®). The detection limits (3 S/N) were calculated according to Long and Winefordner [46], whereas N was expressed as SD of noise determined in the signal domain unless stated otherwise.

3 Results and discussion

3.1 Electrochemical, spectrophotometric, and mass spectrometric characteristics of Zn(II) enclosed in liposomes

In this study, modifying the phospholipid membrane of liposomes containing zinc(II) ions with AuNPs due to targeted anchoring to a target cell or virion was the main aim. Given

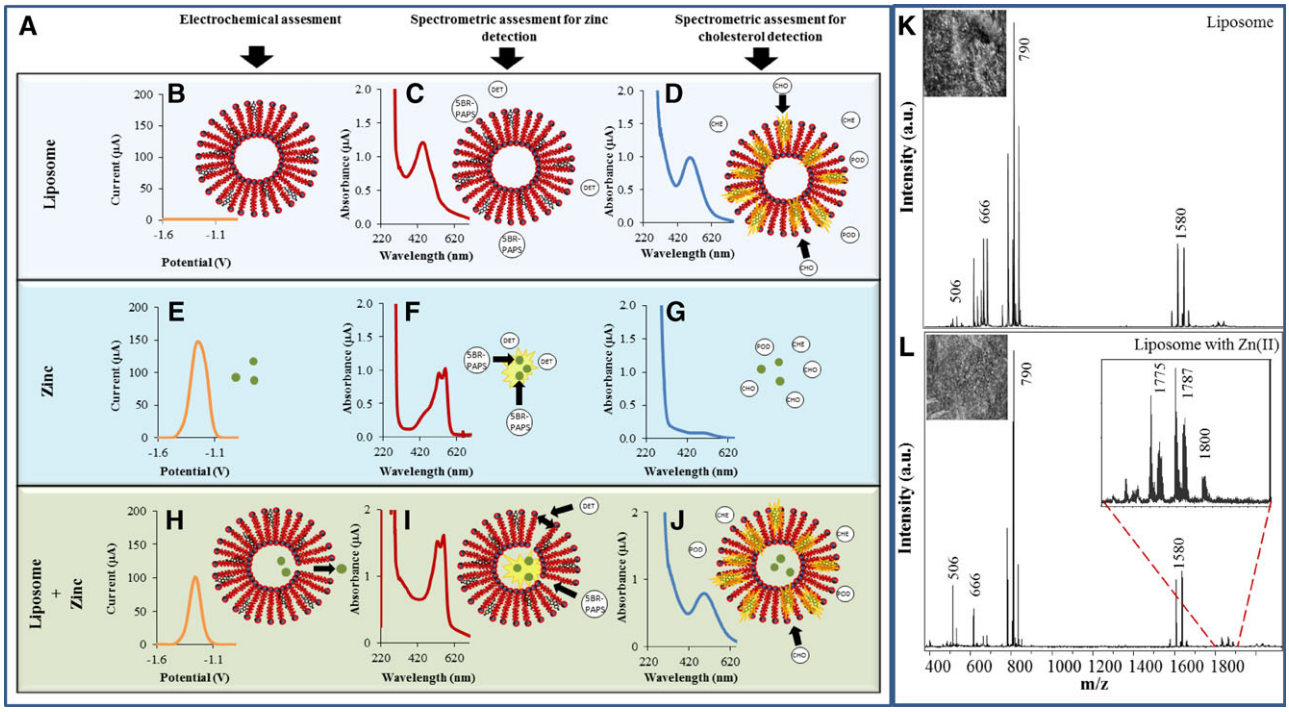

Figure 1. (A) Characteristics of liposome with or without Zn(II) using DPV and spectrophotometry (all solutions were analyzed in 0.2 M acetate buffer of pH 5, spectrophotometry scan was carried out within the range from 220 to 650 nm). Analysis of liposome based on Zn detection by (B) DPV and (C) spectrophotometry, and (D) based on cholesterol by spectrophotometry. (E) Analysis of Zn (300 μM) by DPV and (F) spectrophotometry, and (G) based on cholesterol by spectrophotometry. Analysis of the mixture of liposome with Zn by (H) DPV and (I) spectrophotometry, and (J) based on cholesterol by spectrophotometry. Mass spectra of (K) liposome and (L) mixture of liposome with Zn(II) measured using MALDI-TOF (2,5-dihydroxybenzoic acid was used as a matrix).

the fact that Zn(II) ions are nontoxic, readily available, and easily electrochemically detectable, these were selected as a suitable electrochemical marker [47]. In our experiment, electrochemical and spectrophotometric properties of each component of the prepared nanotransporter were firstly analyzed. Therefore, liposome without zinc was primarily studied and characterized. There were not found liposome electrochemical signal in the potential window of interest selected based on the known electrochemical properties of zinc(II) using DPV (Fig. 1A). In addition, zinc(II) was not detected by spectrophotometric color reaction. Characteristic signal reagent for the determination of zinc, which has an absorption maximum at 437 nm, was only spectrophotometrically detected (Fig. 1B). Cholesterol and phosphorus as components of the liposome were also spectrophotometrically detected (Fig. 1C). Free Zn(II) gave electrochemical signal at potential of −1.2 V (Fig. 1D). Moreover, we were able to detect its red product with used reagent (Nitro-PAPS), which showed an absorption maximum at 555 nm (Fig. 1E). According to our assumption, Zn(II) without reagent was not detected as well as the presence of cholesterol or phosphorus in the solution containing only Zn(II) (Fig. 1F). As the next step, we enclosed Zn(II) into the liposome. The enclosed Zn(II) in liposomes (lipoZn) was electrochemically detected in the same manner as free Zn(II). At the electrochemical detection of Zn(II), the reduction signal is measured; under reducing potential, Zn(II) is reduced to Zn(0) and receives electrons from the working electrode. We were able to demonstrate that liposomes with enclosed Zn(II) gave Zn(II) signal at the potential approximately −1.2 V (Fig. 1G) as in the case of free Zn(II). The theory of electrochemical metal nucleation considering nonstationary effects due to the activation of latent nucleation sites has been successfully translated and applied to describe phenomena observed on lipid membranes. This rather unexpected connection is merely formal, but has resulted in a completely new approach in liposome research. It has been proposed that hydrophobic active sites spontaneously and constantly appear and disappear on lipid membranes. These sites control the affinity of liposomes for hydrophobic surfaces and determine the permeability of the lipid membrane to small hydrophilic molecules [48]. Further, we aimed out attention at spectrophotometric analysis of lipoZn. Zinc liposome interacted with the reagent for determination of zinc(II) and the resulted colored product had absorption maximum at 555 nm (Fig. 1H). The opening of lipoZn caused detergent presented in the reagent used for determination of zinc(II). Spectrophotometric test for the presence of cholesterol and phosphorus revealed the presence of both components of the liposome, even after the addition of Zn(II) (Fig. 1I).

MALDI-TOF was used to characterize liposomes with and without Zn(II). The MALDI-TOF spectra showed distinct peaks corresponding to the parts of liposomes (Fig. 1J). The main signals were identified at 790.79 and 1580.38 *m/z*, in both spectra with and/or without Zn(II) ions. The signal

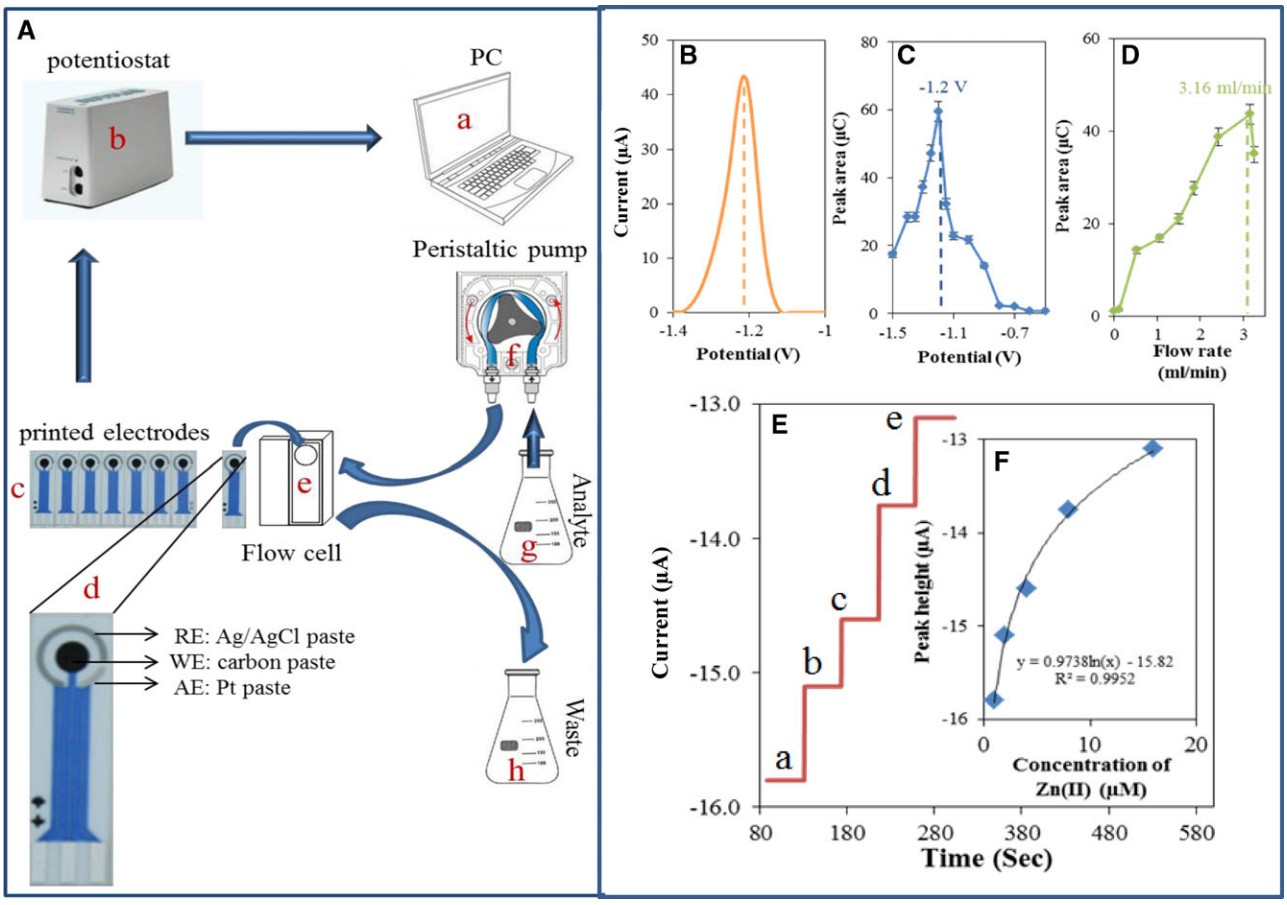

Figure 2. (A) The scheme of the microfluidic system connections, a = personal computer with NOVA 1.8 software installed, b = mobile potentiostat unit PGSTAT 101, c = disposable screen printed sensors (electrodes), d = detail of sensor with three-electrode connection (RE: Ag/AgCl paste, WE: carbon paste, AE: Pt paste), e = scheme of flow cell as housing for the electrodes, f = peristaltic pump (Amersham Biosciences), g = sample for analysis and h = waste. (B) DP voltammograms of lipoZn. (C) Hydrodynamic voltammogram of lipoZn. (D) Dependence of peak height measured at potential −1.2 V on the flow rate 0.2 M acetate buffer of pH 5. (E) Amperometric change of the reduction signal of lipoZn according to concentration a = 10 μM, b = 20 μM, c = 40 μM, d = 80 μM, e = 160 μM (applied potential − 1.2 V).

790.79 *m/z* corresponded to the 1,2-dioleoyl-*sn*-glycero-3-phospho-rac-(1-glycerol) or phosphatidylcholine, which are the main components of liposome. The signal 1580.38 *m/z* corresponded to phospholipid dimers. The similar results of MALDI-TOF analysis of Coatsome liposomes were discussed by Helsper et al. [49]. The main MALDI-TOF signals of Coatsome liposomes were phospholipids dipalmitoylphosphatidylglycerol and its dimer. The results of the analysis of liposomes with encapsulated Zn(II) showed a new peak at *m/z* 1775.51 next to peak *m/z* 1580.38. Zn(II) ion mass is 65.38 Da; therefore, this new peak corresponded to the sum of phospholipid dimer and approximately three of Zn(II) ions per complex.

3.2 Optimizing of detection of zinc liposome using microfluidic system

Microfluidic devices have many advantages compared to their macroscale counterparts, including a reduced reaction solution and cell consumption, an improved analysis speed, a greater portability, a greater sensitivity, lower fabrication and operating costs, and the potential for parallel processing and integration with other miniaturized devices [50, 51]. The suggested method utilizes a flow cell (with a total volume of 50 μL) in combination with screen-printed electrochemical sensors (Fig. 2A). As it is shown in Fig. 1, zinc was well electrochemically analyzable in liposome. A shift was observed in the peak (1199 ± 0.001 V, n = 5, RSD = 0.8%, Fig. 2B) for 10 mV to more positive potential only in comparison with signal of free Zn(II). The detection limit (3 S/N) of Zn(II) enclosed in liposome was estimated as 100 nM Zn(II). The calibration curve was linear from 0.5 to 340 μM Zn(II) with R^2 = 0.9976, (Table 1). In the case of production of one-purpose device, it is beneficial to apply amperometric detection. The basic amperometric analysis includes measuring hydrodynamic voltammograms [52], which we also measured. In this case, the selected potentials were −1.6, −1.5, −1.4, −1.3, −1.25, −1.15, −1.1, −0.9, −0.8, −0.7, −0.6, and −0.5 V at a flow of electrolyte 2 mL/min. The obtained and

Table 1. Analytical parameters of electrochemical determination of Zn(II) in LipoZn

Substance	Regression equation	Linear dynamic range (μM)	$R^{2a)}$	LOD[b)] (μM)	LOQ[c)] (μM)	RSD (%)
Zn(II)	$y = 0.4769x$	0.5–343.4	0.997	0.5	10	8.2

a) Coefficient of determination.
b) 3 S/N.
c) 10 S/N.

typical hydrodynamic voltammogram is shown in Fig. 2C. One very sharp peak at the potential of −1.2 V (reduction of zinc ions) and a second maximum at the potential of −0.9 V (possibly reduction of zinc(II) ions bound to the surface of the outer membrane) were observed in the voltammogram). Flow rate of mobile phase (electrolyte) significantly affects the electrochemical signals as discussed previously [53]. The obtained dependence lipoZn peak height on the flow rate of the electrolyte is shown in Fig. 2D. Higher flow rates resulted in a marked increase in detected signal. Flow rate 0.5 mL/min enhanced signal of lipoZn more than 30%. From 1 to 3 mL/min, the signal of lipoZn increased in a linear trend. Flow rate higher than 3 mL/min led to a decrease in the signal of 10% (Fig. 2D). Further, peak height dependence on varying concentration of lipoZn (1–160 μM) at a constant potential of −1.2 V and a flow rate of 3 mL/min was studied. The increasing concentration of lipoZn was recorded as step-growth reduction signal of Zn(II) at the time of 85–300 s (Fig. 2E). Height of the reduction peak had logarithmic course ($n = 5$, RSD = 5.9%) and it is shown in Fig. 2F.

After that, we electrochemically characterized lipoZn using microfluidic device and found that we were able to use this device for analysis of lipoZn. We were interested in the optimization of lipoZn preparation. Therefore, four types of liposomes (lipoZn1, lipoZn2, lipoZn3, and lipoZn4) were tested to ensure the highest amount of the Zn(II) enclosed into the liposome. Applied concentration of Zn(II) for the preparation of lipoZn was within the range from 0.1 to 60 mM. Unclosed Zn(II) was removed using a microdialysis column. Using AAS and electrochemical detection, it was demonstrated that it was possible to enclose maximally 2.72 mM Zn(II) under the application 30.58 mM Zn(II) into the liposome. Higher applied concentration (>30.58 mM) of Zn(II) caused the precipitation of the sample. Differences between various lipoZn are shown in Tables 2 and 3. It clearly follows from the results obtained that the percentage of Zn(II) incorporated in the liposome decreased with the increasing concentrations of applied Zn(II). One may suggest that there is limitation in the cavity of liposomes (Fig. 3A). In addition, microfluidic DPV analysis was able to demonstrate that the peak potential of lipoZn shifted the negative potentials with decreasing concentrations of Zn(II) in the zinc-liposome complex (Fig. 3B and D), and the method could be, therefore, useful for determining not only the amount of encapsulated Zn(II) into liposomes but also for verifying the stability of the complex and the ratio of liposome/Zn (further details will be published elsewhere). As we mentioned above, AAS was also used for determination of zinc(II) in lipoZn complexes. Both the methods were correlated (Fig. 3C). The results correlated and both methods are suitable for monitoring Zn(II) contained in the liposome.

In addition, enclosed Zn(II) in liposomes was also studied using UV/Vis spectrophotometry. Thereaction of zinc liposome with the reagent (Nitro-PAPS) used for the determination of zinc was studied. SDS (0.05%, w/w) was used for the opening of the liposomes. It clearly follows from the results obtained that the increasing concentration of Zn(II) in the liposomes enhanced spectrophotometric signal, which corresponded to the reaction of Zn(II) with an agent Nitro-PAPS with absorption maximum 555 nm (Fig. 3E-a, F-b, G-c, and H-d). It was clearly demonstrated that Zn(II) was enclosed in liposomes and we were able measure it using three independent methods.

3.3 The design of nanodevices for targeted transport

Previously prepared and characterized lipoZn was further modified with AuNPs. We wanted to anchor the lipoZn specifically to a predefined surface. For this purpose, we used the method according Bhuvana et al. [38]. After modifying the surface of the liposome with AuNPs, white lipoZn color changed to a light purple. The presence of AuNPs on the surface of the liposome was demonstrated by AAS with a total gold content as 0.50 ± 0.05 μg/mL lipoZn ($n = 5$, RSD = 2%). It is well known that gold has a strong affinity to SH

Table 2. Determination of zinc using AAS in four types of liposomes prepared with different concentration of Zn(II) ($n = 5$)

	LipoZn 1	LipoZn 2	LipoZn 3	LipoZn 4
Applied Zn (mM)	3.82	7.65	15.29	30.58
Encapsulated Zn (mM)	1.4 ± 0.1	2.5 ± 0.1	2.6 ± 0.1	2.7 ± 0.2
Percentage of encapsulated Zn	36.4	32.5	17.3	8.9

Table 3. Determination of zinc using DPV in four types of liposomes prepared with different concentration of Zn(II) ($n = 5$)

	LipoZn 1	LipoZn 2	LipoZn 3	LipoZn 4
Applied Zn (mM)	3.82	7.65	15.29	30.58
Encapsulated Zn (mM)	1.3 ± 0.1	1.8 ± 0.1	2.0 ± 0.2	2.2 ± 0.1
Percentage of encapsulated Zn	33.0	23.4	13.0	7.0

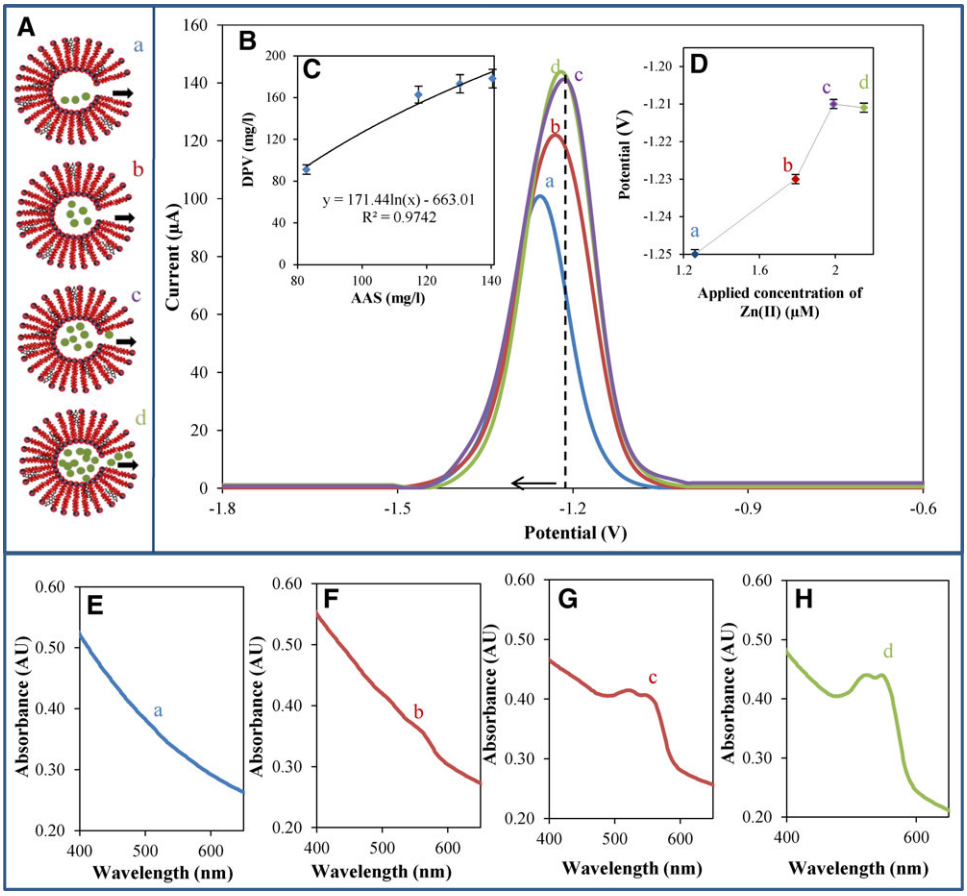

Figure 3. (A) Scheme of four prepared variants of liposomes (LipoZn1, LipoZn 2, LipoZn 3, and LipoZn4) with different Zn(II) concentrations enclosed inside (a = 1.39 mM Zn(II), b = 2.49 mM Zn(II), c = 2.64 mM Zn(II), and d = 2.72 mM Zn(II)). (B) DPV of Zn(II) released from liposomes using addition of SDS (0.05% w/w), a = 1.26 mM Zn(II), b = 1.79 mM Zn(II), c = 1.99 mM Zn(II), d = 2.15 mM Zn(II). (C) Correlation of Zn(II) determined by DPV and AAS. (D) The influence of various applied Zn(II) concentrations of the potential of peak of lipoZn. Spectrophotometric records of the complexes of 0.02 mM Nitro-PAPS with Zn(II) released from liposomes in original concentrations (E) a = 1.39 mM Zn(II), (F) b = 2.49 mM Zn(II), (G) c = 2.64 mM Zn(II), and (H) d = 2.72 mM Zn(II).

moieties. Therefore, we focused on the use of the advantage of the great affinity of AuNPs to ODN-SH, as part of the anchoring system of the nanotransportér (Fig. 4A). In this way, we had a tool for targeted anchoring of the prepared lipoZn-AuNPs-SH to other target molecules (tumor cell, the viral receptor, etc.). To test the functionality of the suggested nanotransporter system, binding of the complementary ODN adenine sequence was used. Using this approach, it was possible to hybridize the whole complex to magnetic beads (MB, DBT25) using TTTTT and AAAAA complementarity. Liposomal carrier lipoZn-AuNPs-SH-ODN-ODN-MB was prepared (Fig. 4A). Multifunctional envelope-type nanodevices are very promising nonviral gene delivery vectors because they are biocompatible and enable programmed packaging of various functional elements into an individual nanostructured liposome [2], with subsequent use for lab, on a chip technology [54, 55].

3.4 Electrochemical and UV/Vis spectrophotometric characteristics of nanotrasporter (LipoZn-AuNPs-SH-ODN-ODN-MB complex)

Targeted delivery of bioactive substances (drugs, DNA, peptides, fluorescence, and electrochemical labels) allows a wide range of applications. Liposomes were widely utilized as carriers of molecules in the fields of nanodevices, drug delivery, and gene delivery, as well as a mimic for cell membranes [18, 56]. DNA or RNA molecule encapsulated in the solution in liposomes stay unchanged longer compared to DNA or RNA in an ordinary buffer solution where rapid degradation of nucleic acids occurs [57]. Encapsulation of DNA or RNA molecules in liposomes increases the possibilities of endocytosis; therefore, liposomes are suitable as a tool of gene therapy [58–60]. Wu et al. investigated the antitumor activity of microRNA incorporated in liposomes with tumor suppressor miR-133b against lung cancer of mice. In the case of mice treated with these liposomes, the expression of miR-133b in the lungs was 52-fold higher in comparison with untreated mice [61]. In the next work, Rhee et al. formulated an efficacious peptide vaccine without carriers using phosphodiester CpG-DNA and a special liposome complex [62]. Potential epitope peptides predicted from the hemagglutinin protein of the H5N1 were used to immunize mice. Immunization with a complex of the cell epitope and lipoplex completely protects mice challenged with a lethal dose of recombinant H5N1 virus. Recently, biomarkers for the quantitative view of pancreatic cancer cells based on quantum dots enclosed in liposomes were also described [63].

In this experiment, we focused on the characterization of complex formed (nanodevices), which can be used for targeted delivering of the mentioned substances. According

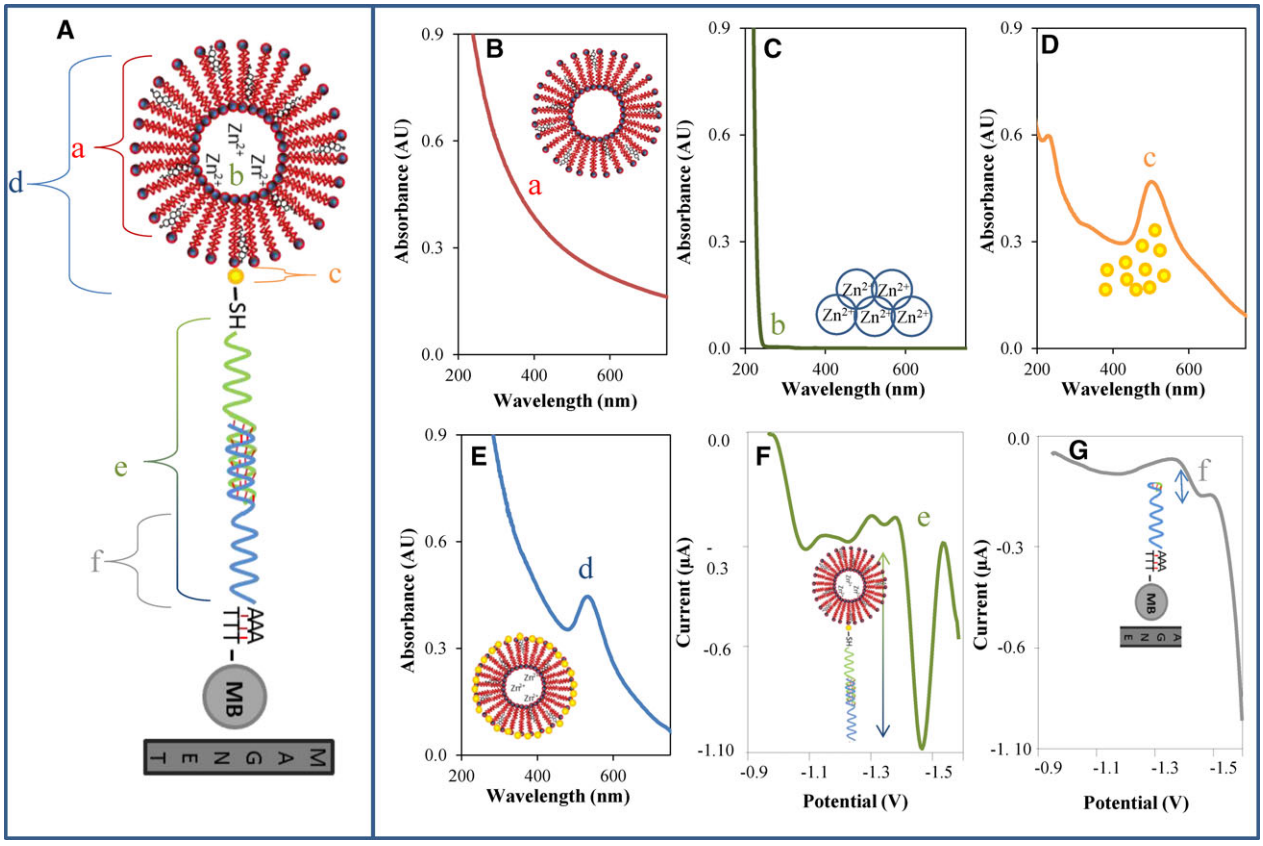

Figure 4. Characterization of liposomal carrier using spectrophotometry and square-wave voltammetry. (A) Scheme of lipoZn carrier and its anchoring to the magnetizable particle, a = liposome comprising from phospholipid bilayer with an inner cavity, b = zinc in the cavity, c = AuNPs bound to the surface liposome, d = AuNPs modified with zinc liposome (lipoZn-AuNPS-SH), e = oligonucleotide bound with SH groups on the AuNP and coupled with a complementary oligonucleotide, f = complementary oligonucleotide used to anchor lipoZn-AuNPS-SH-ODN-ODN to magnetic particles (MB). (B), (C), (D), and (E) UV/Vis spectrophotometric records measured within the range from 200 to 650 nm of a = liposome, b = 20 mM zinc nitrate, c = 0.5 mM AuNPs, and d = lipoZn modified with AuNPs (0.5 mM). (F and G) e = square-wave voltammetry electrochemical signal oligonucleotide bound with SH group lipoZn-AuNPS, f = complementary oligonucleotide anchor studied complex to MB.

to previous chapters, transporter (LipoZn-AuNPs-SH-ODN-ODN-MB complex) was created (Fig. 4A). This complex consisted of a liposome (lipoZn, Fig. 4A-a), which had enclosed Zn(II) in its cavity (Fig. 4A-b) and AuNPs on its surface (phospholipid bilayer) to form AuNPs-lipoZn (Fig. 4A-c). Oligonucleotides were bound to AuNPs (lipoZn-AuNPs-SH-ODN) using SH groups (Fig. 4A-e). The created lipoZn-AuNPs-SH-ODN transporter was isolated using magnetizable particles (MB) with immobilized complementary oligonucleotides (ODN-MB) according to Fig. 4A-f. The individual components of the complex were spectrophotometrically and electrochemically studied. UV/Vis analysis of liposome (Fig. 4B) and free Zn(II) (Fig. 4C) showed absorption maximum. In the same way, AuNPs were studied. Spectrophotometric record showed two absorption maxima, in the UV (230 nm) and Vis (500 nm) region (Fig. 4D). Spectrophotometric record of lipoZn modified with AuNPs (AuNPs-lipoZn) demonstrated complex formation between liposome and AuNPs. Interaction among AuNPs and lipoZn resulted in a shift of absorption maxima AuNPs (500 nm) into Vis region for 34 nm (534 nm = lipoZn-AuNPs, Fig. 4E). AuNPs-modified lipoZn (lipoZn-AuNPs) was mixed with oligonucleotides (ODN-SH) that were hybridized to complementary oligonucleotides bound to magnetic beads (MB-ODN). The binding was electrochemically detected by square-wave voltammetry based on reducing signal of nucleic acid called CA (cytosine and adenine) peak at −1.45 V [64]. The observed electrochemical signal corresponded to the used complementary oligonucleotides (Fig. 4F). In the same way, oligonucleotide binding to magnetizable particles (without binding to the liposome) was confirmed, which showed specific (weaker) electrochemical signal (Fig. 4G). Oligonucleotide binding to the surface and creating lipoZn-AuNPs-SH-ODN-ODN-MB was very fast and selective.

3.5 Electrochemical microfluidic detection of zinc(II) after the isolation of zinc liposome by use of magnetizable particles

Magnetizable nano- and microparticles are widely used in the isolation of various substances. The advantage of such particles is their easy modification to achieve specific binding.

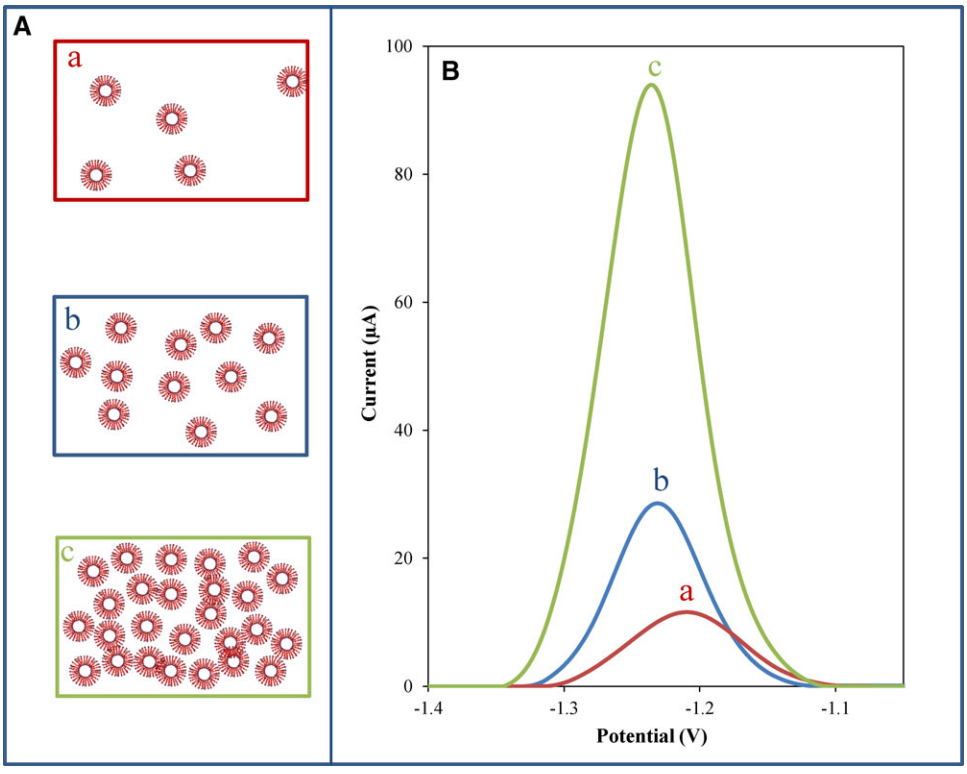

Figure 5. Analysis of three samples of lipoZn isolated using magnetizable particles with various concentration of oligonucleotide as a = 10 μg/mL, b = 40 μg/mL, and c = 80 μg/mL to form a complex lipoZn-AuNPs-SH-ODN. (A) Schematic representation of a = 1.2×10^{12} liposomes per milliliters, b = 7.2×10^{12} liposomes per milliliters, and c = 24.1×10^{12} liposomes per milliliters. (B) Electrochemical signal measured by DPV of Zn(II) in a = 1.2×10^{12} liposomes per milliliters, b = 7.2×10^{12} liposomes per milliliters, and c = 24.1×10^{12} liposomes per milliliters isolated using magnetizable particles prepared with different concentrations of oligonucleotides, a = 10 μM, b = 60 μM, and c = 200 μM. Electrochemical signal was observed immediately after elution of the sample at room temperature.

Isolated lipoZn-AuNPs-SH-ODN was investigated electrochemically (DPV) using optimized microfluidic techniques. Primarily, the modified LipoZn was mixed with ODN with final concentration of 10, 40, and 80 μg/mL. Further, magnetizable particles were mixed with complementary oligonucleotide of the final concentration of 100 μg/mL. Subsequently, lipoZn-AuNPs-SH-ODN was isolated by using MB. The optimized microfluidic analysis showed that decreasing concentration of nucleotides bound via SH groups to lipoZn-AuNPs-SH-ODN decreased the number of isolated lipoZn. The decreasing trend in the zinc reduction signal depending on the decreasing concentration of oligonucleotide bound to lipoZn is shown in Fig. 5B (a = 200 μM Zn(II), b = 60 μM Zn(II) and c = 10 μM Zn(II)). It was calculated on the basis of the concentration of Zn contained in liposomes and liposome average volume with a diameter of 200 nm [65] that the liposome could encapsulate 5000 Zn(II) ions. After recalculation of concentration-specified zinc liposome, it was estimated (assuming that a liposome contains an average of 5000 atoms of Zn(II)) that we isolated a = 1.2×10^{12}, b = 7.2×10^{12}, and c = 24.1×10^{12} liposomes per milliliters.

4 Concluding remarks

In this study, nanodevice for targeted delivery was suggested. As the transporter, zinc-containing liposome, which was modified with AuNPs and served to establish the oligonucleotide binding, was used. This nanodevice was anchored to a magnetizable particle with a complementary oligonucleotide. Functionality of the nanodevices was proven through electrochemically and spectrometric determination of Zn(II) enclosed in liposomes. Designed nanotransporter may also be used for targeted and controlled transport to specific tissues (tumor) and to prevent the multiplication of viruses [66–68]. Besides this, magnetic nanoparticle clusters, which can, under the influence of an external magnet, target both the tumor and its microenvironment, may be also enclosed [69].

The financial support from the following projects NanoBioTECell GACR P102/11/1068 and CEITEC CZ.1.05/1.1.00/02.0068 is highly acknowledged. The authors wish to express their thanks to Martina Stankova for perfect technical assistance and to Jan Prasek for electrode preparation.

The authors have declared no conflict of interest.

5 References

[1] Kwakye, S., Goral, V. N., Baeumner, A. J., *Biosens. Bioelectron.* 2006, *21*, 2217–2223.

[2] Kitazoe, K., Park, Y. S., Kaji, N., Okamoto, Y., Tokeshi, M., Kogure, K., Harashima, H., Baba, Y., *PLoS One* 2012, *7*, e39057.

[3] Sia, S. K., Whitesides, G. M., *Electrophoresis* 2003, *24*, 3563–3576.

[4] Lei, K. F., *JALA* 2012, *17*, 330–347.

[5] Atalay, Y. T., Vermeir, S., Witters, D., Vergauwe, N., Verbruggen, B., Verboven, P., Nicolai, B. M., Lammertyn, J., *Trends Food Sci. Technol.* 2011, *22*, 386–404.

[6] Eicher, D., Merten, C. A., *Expert Rev. Mol. Diagn.* 2011, *11*, 505–519.

[7] Giridharan, V., Yun, Y., Hajdu, P., Conforti, L., Collins, B., Jang, Y., Sankar, J., *J. Nanomater.* 2012, *2012*, 789841.

[8] Ricciardi, C., Canavese, G., Castagna, R., Ferrante, I., Ricci, A., Marasso, S. L., Napione, L., Bussolino, F., *Biosens. Bioelectron.* 2010, *26*, 1565–1570.

[9] Huang, Y., Shi, M., Zhao, S. L., Liang, H., *Electrophoresis* 2011, *32*, 3196–3200.

[10] Weiss, V. U., Bilek, G., Pickl-Herk, A., Blaas, D., Kenndler, E., *Electrophoresis* 2009, *30*, 2123–2128.

[11] Viswanathan, S., Rani, C., Anand, A. V., Ho, J. A. A., *Biosens. Bioelectron.* 2009, *24*, 1984–1989.

[12] Nugen, S. R., Asiello, P. J., Connelly, J. T., Baeumner, A. J., *Biosens. Bioelectron.* 2009, *24*, 2428–2433.

[13] Chen, W. Y., Chen, H. C., Yang, Y. S., Huang, C. J., Chan, H. W. H., Hu, W. P., *Biosens. Bioelectron.* 2013, *41*, 795–801.

[14] Zhong, Z. Y., Peng, N., Qing, Y., Shan, J. L., Li, M. X., Guan, W., Dai, N., Gu, X. Q., Wang, D., *Electrochim. Acta* 2011, *56*, 5624–5629.

[15] Viswanathan, S., Wu, L. C., Huang, M. R., Ho, J. A. A., *Anal. Chem.* 2006, *78*, 1115–1121.

[16] Li, J. P., Li, S. H., Yang, C. F., *Electroanalysis* 2012, *24*, 2213–2229.

[17] Nam, J. M., Thaxton, C. S., Mirkin, C. A., *Science* 2003, *301*, 1884–1886.

[18] Liu, Q. T., Boyd, B. J., *Analyst* 2013, *138*, 391–409.

[19] Edwards, K. A., Bolduc, O. R., Baeumner, A. J., *Curr. Opin. Chem. Biol.* 2012, *16*, 444–452.

[20] Akbarzadeh, A., Rezaei-Sadabady, R., Davaran, S., Joo, S. W., Zarghami, N., Hanifehpour, Y., Samiei, M., Kouhi, M., Nejati-Koshki, K., *Nanoscale Res. Lett.* 2013, *8*, 102.

[21] Sharma, A., Sharma, U. S., *Int. J. Pharm.* 1997, *154*, 123–140.

[22] Dos Santos, N., Waterhouse, D., Masin, D., Tardi, P. G., Karlsson, G., Edwards, K., Bally, M. B., *J. Control. Release* 2005, *105*, 89–105.

[23] Pantos, A., Tsiourvas, D., Paleos, C. M., Nounesis, G., *Langmuir* 2005, *21*, 6696–6702.

[24] Boulikas, T., *Oncol. Rep.* 2004, *12*, 3–12.

[25] Locascio, L. E., Hong, J. S., Gaitan, M., *Electrophoresis* 2002, *23*, 799–804.

[26] Ho, J. A. A., Hsu, H. W., *Anal. Chem.* 2003, *75*, 4330–4334.

[27] Vamvakaki, V., Fournier, D., Chaniotakis, N. A., *Biosens. Bioelectron.* 2005, *21*, 384–388.

[28] Oja, C., Tardi, P., Schutze-Redelmeier, M. P., Cullis, P. R., *Biochim. Biophys. Acta Biomembr.* 2000, *1468*, 31–40.

[29] Petersen, A. L., Hansen, A. E., Gabizon, A., Andresen, T. L., *Adv. Drug Deliv. Rev.* 2012, *64*, 1417–1435.

[30] Ge, S. G., Jiao, X. L., Chen, D. R., *Analyst* 2012, *137*, 4440–4447.

[31] Qu, B., Guo, L., Chu, X., Wu, D. H., Shen, G. L., Yu, R. Q., *Anal. Chim. Acta* 2010, *663*, 147–152.

[32] Sunamoto, J., Shironita, M., Kawauchi, N., *Bull. Chem. Soc. Jpn.* 1980, *53*, 2778–2781.

[33] Nomura, F., Nagata, M., Inaba, T., Hiramatsu, H., Hotani, H., Takiguchi, K., *Proc. Natl. Acad. Sci. U S A* 2001, *98*, 2340–2345.

[34] Matsumura, H., Neytchev, V., Terezova, N., Tsoneva, I., *Colloid Surf. B Biointerfaces* 2004, *33*, 243–249.

[35] Kimling, J., Maier, M., Okenve, B., Kotaidis, V., Ballot, H., Plech, A., *J. Phys. Chem. B* 2006, *110*, 15700–15707.

[36] Polte, J., Ahner, T. T., Delissen, F., Sokolov, S., Emmerling, F., Thunemann, A. F., Kraehnert, R., *J. Am. Chem. Soc.* 2010, *132*, 1296–1301.

[37] Kunjachan, S., Blauz, A., Mockel, D., Theek, B., Kiessling, F., Etrych, T., Ulbrich, K., van Bloois, L., Storm, G., Bartosz, G., Rychlik, B., Lammers, T., *Eur. J. Pharm. Sci.* 2012, *45*, 421–428.

[38] Bhuvana, M., Narayanan, J. S., Dharuman, V., Teng, W., Hahn, J. H., Jayakumar, K., *Biosens. Bioelectron.* 2013, *41*, 802–808.

[39] Huska, D., Hubalek, J., Adam, V., Vajtr, D., Horna, A., Trnkova, L., Havel, L., Kizek, R., *Talanta* 2009, *79*, 402–411.

[40] Krejcova, L., Dospivova, D., Ryvolova, M., Kopel, P., Hynek, D., Krizkova, S., Hubalek, J., Adam, V., Kizek, R., *Electrophoresis* 2012, *33*, 3195–3204.

[41] Krizkova, S., Jilkova, E., Krejcova, L., Cernei, N., Hynek, D., Ruttkay-Nedecky, B., Sochor, J., Kynicky, J., Adam, V., Kizek, R., *Electrophoresis* 2013, *34*, 224–234.

[42] Krizkova, S., Ryvolova, M., Hynek, D., Eckschlager, T., Hodek, P., Masarik, M., Adam, V., Kizek, R., *Electrophoresis* 2012, *33*, 1824–1832.

[43] Zitka, O., Krizkova, S., Krejcova, L., Hynek, D., Gumulec, J., Masarik, M., Sochor, J., Adam, V., Hubalek, J., Trnkova, L., Kizek, R., *Electrophoresis* 2011, *32*, 3207–3220.

[44] Prasek, J., Trnkova, L., Gablech, I., Businova, P., Drbohlavova, J., Chomoucka, J., Adam, V., Kizek, R., Hubalek, J., *Int. J. Electrochem. Sci.* 2012, *7*, 1785–1801.

[45] Chudobova, D., Dobes, J., Nejdl, L., Maskova, D., Merlos Rodrigo, M. A., Ruttkay-Nedecky, B., Zitka, O., Krystofova, O., Kynicky, J., Konecna, M., Pohanka, M., Hubalek, J., Zehnalek, J., Klejdus, B., Kizek, R., Adam, V., *Int. J. Electrochem. Sci.* 2013, *8*, 4422–4440.

[46] Long, G. L., Winefordner, J. D., *Anal. Chem.* 1983, *55*, A712-A724.

[47] Cummings, J. E., Kovacic, J. P., *J. Vet. Emerg. Crit. Care* 2009, *19*, 215–240.

[48] Hernandez, V. A., *J. Solid State Electrochem.* 2013, *17*, 299–305.

[49] Helsper, J., Peters, R. J. B., Brouwer, L., Weigel, S., *Anal. Bioanal. Chem.* 2013, *405*, 1181–1189.

[50] Young, J., *Forbes* 1996, *158*, 210–211.

[51] Rios, A., Zougagh, M., Avila, M., *Anal. Chim. Acta* 2012, *740*, 1–11.

[52] Zitka, O., Kominkova, M., Skalickova, S., Skutkova, H., Provaznik, I., Eckschlager, T., Stiborova, M., Adam, V., Trnkova, L., Kizek, R., *Int. J. Electrochem. Sci.* 2012, *7*, 10544–10561.

[53] Zitka, O., Skutkova, H., Krystofova, O., Sobrova, P., Adam, V., Zehnalek, J., Havel, L., Beklova, M., Hubalek, J., Provaznik, I., Kizek, R., *Int. J. Electrochem. Sci.* 2011, *6*, 1367–1381.

[54] Peyman, S. A., Abou-Saleh, R. H., McLaughlan, J. R., Ingram, N., Johnson, B. R. G., Critchley, K., Freear, S., Evans, J. A., Markham, A. F., Coletta, P. L., Evans, S. D., *Lab. Chip* 2012, *12*, 4544–4552.

[55] Birnbaumer, G., Kupcu, S., Jungreuthmayer, C., Richter, L., Vorauer-Uhl, K., Wagner, A., Valenta, C., Sleytr, U., Ertl, P., *Lab. Chip* 2011, *11*, 2753–2762.

[56] Livney, Y. D., *Curr. Opin. Colloid Interface Sci.* 2010, *15*, 73–83.

[57] Oberle, V., Bakowsky, U., Zuhorn, I. S., Hoekstra, D., *Biophys. J.* 2000, *79*, 1447–1454.

[58] Xu, Y. H., Szoka, F. C., *Biochemistry* 1996, *35*, 5616–5623.

[59] Szoka, F. C., *Biotechnol. Appl. Biochem.* 1990, *12*, 496–500.

[60] Koltover, I., Salditt, T., Radler, J. O., Safinya, C. R., *Science* 1998, *281*, 78–81.

[61] Wu, Y., Crawford, M., Yu, B., Mao, Y. C., Nana-Sinkam, S. P., Lee, L. J., *Mol. Pharm.* 2011, *8*, 1381–1389.

[62] Rhee, J. W., Kim, D., Park, B. K., Kwon, S., Cho, S., Lee, I., Park, M. S., Seo, J. N., Kim, Y. S., Choi, H. S., Lee, Y., Kwon, H. J., *PLoS One* 2012, *7*, e48750.

[63] Lee, K. H., Galloway, J. F., Park, J., Dvoracek, C. M., Dallas, M., Konstantopoulos, K., Maitra, A., Searson, P. C., *Nanomedicine* 2012, *8*, 1043–1051.

[64] Huska, D., Hubalek, J., Adam, V., Kizek, R., *Electrophoresis* 2008, *29*, 4964–4971.

[65] Kato, K., Koido, M., Kobayashi, M., Akagi, T., Ichiki, T., *Electrophoresis* 2013, *34*, 1212–1218.

[66] Swaminathan, J., Ehrhardt, C., *Expert Opin. Drug Deliv.* 2012, *9*, 1489–1503.

[67] Miyako, E., Kono, K., Yuba, E., Hosokawa, C., Nagai, H., Hagihara, Y., *Nat. Commun.* 2012, *3*, 1226.

[68] van Kouwenhove, M., Kedde, M., Agami, R., *Nat. Rev. Cancer* 2011, *11*, 644–656.

[69] Mikhaylov, G., Mikac, U., Magaeva, A. A., Itin, V. I., Naiden, E. P., Psakhye, I., Babes, L., Reinheckel, T., Peters, C., Zeiser, R., Bogyo, M., Turk, V., Psakhye, S. G., Turk, B., Vasiljeva, O., *Nat. Nanotechnol.* 2011, *6*, 594–602.

